Journal of Colloid and Interface Science 610 (2022) 321–333

Contents lists available at ScienceDirect

Journal of Colloid and Interface Science

journal homepage: www.elsevier.com/locate/jcis

Antibacterial nanofibers of pullulan/tetracycline-cyclodextrin inclusion complexes for Fast-Disintegrating oral drug delivery

Emmy Hsiung [a,1], Asli Celebioglu [a,*,1], Rimi Chowdhury [b], Mehmet E. Kilic [c], Engin Durgun [d], Craig Altier [b], Tamer Uyar [a,*]

[a] Fiber Science Program, Department of Human Centered Design, College of Human Ecology, Cornell University, Ithaca, NY 14853, United States
[b] Department of Population Medicine and Diagnostic Sciences, College of Veterinary Medicine, Cornell University, Ithaca, NY 14850, United States
[c] Computational Science Research Center, Korea Institute of Science and Technology, Seoul 02792, Republic of Korea
[d] UNAM- National Nanotechnology Research Center and Institute of Materials Science and Nanotechnology, Bilkent University, Ankara 06800, Turkey

HIGHLIGHTS

- Pullulan/tetracycline-CD-IC nanofibers were generated via electrospinning.
- Hydroxypropyl-β-CD (HPβCD) was used for inclusion complex (IC) formation.
- The inclusion complex formation was confirmed by ab initio modelling study.
- Pullulan/tetracycline-CD-IC nanofibers disintegrated rapidly in artificial saliva.
- Tetracycline-HPβCD-IC provided enhanced release and antibacterial property.

GRAPHICAL ABSTRACT

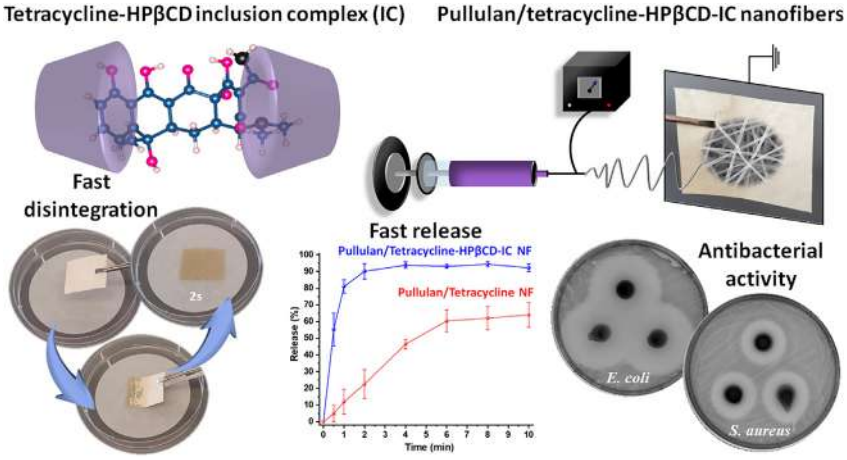

ARTICLE INFO

Article history:
Received 1 October 2021
Revised 1 December 2021
Accepted 3 December 2021
Available online 8 December 2021

Keywords:
Cyclodextrin
Electrospinning
Nanofibers
Inclusion complex
Tetracycline
Antibiotic
Fast disintegrating

ABSTRACT

Tetracycline is a widely used antibiotic suffering from poor water solubility and low bioavailability. Here, hydroxypropyl-beta-cyclodextrin (HPβCD) was used to form inclusion complexes (IC) of tetracycline with 2:1 M ratio (CD:drug). Then, tetracycline-HPβCD-IC was mixed with pullulan- a non-toxic, water-soluble biopolymer - to form nanofibrous webs via electrospinning. The electrospinning of pullulan/tetracycline-HPβCD-IC was yielded into defect-free nanofibers collected in the form of a self-standing and flexible material with the loading capacity of ~ 7.7 % (w/w). Pullulan/tetracycline nanofibers was also generated as control sample having the same drug loading. Tetracycline was found in the amorphous state in case of pullulan/tetracycline-HPβCD nanofibers due to inclusion complexation. Through inclusion complexation with HPβCD, enhanced aqueous solubility and faster release profile were provided for pullulan/tetracycline-HPβCD-IC nanofibers compared to pullulan/tetracycline one. Additionally, pullulan/tetracycline-HPβCD-IC nanofibers readily disintegrated when wetted with artificial saliva while pullulan/tetracycline nanofibers were not completely absorbed by the same simulate environment. Electrospun nanofibers showed promising antibacterial activity against both gram-positive and gram-negative bacteria.

* Corresponding authors.
E-mail addresses: ac2873@cornell.edu (A. Celebioglu), tu46@cornell.edu (T. Uyar).
[1] Contributed equally.

https://doi.org/10.1016/j.jcis.2021.12.013

Fast dissolving
Oral drug delivery
Antibacterial

Briefly, our findings indicated that pullulan/tetracycline-HPβCD-IC nanofibers could be an attractive material as orally fast disintegrating drug delivery system for the desired antibiotic treatment thanks to its promising physicochemical and antibacterial properties.

1. Introduction

Recently, developments in oral fast-disintegrating drug delivery systems have been followed closely in the pharmaceutical industry. Oral dosage, particularly in the form of tablets, are the most common form of drug delivery due to ease of administration, controlled dosages, pain avoidance, etc. [1]. However, large dosage sizes can present problems in pediatric, geriatric, or dysphagic patients who have difficulty with swallowing pills. Fast-dissolving drug delivery systems offer an alternative to swallowing large tablets by letting a solid dosage form (films, patches, tablets) containing medicinal substances rapidly disintegrate on the tongue [2]. Fast-disintegrating systems are also favorable for drugs with low bioavailability, as it avoids first-pass metabolism and thus increases their bioavailability. Other advantages of fast-disintegrating oral systems include administration without water and a lessened choking hazard [1,3].

Incorporating drug molecules into electrospun nanofibers is one method of fabricating fast-disintegrating drug delivery systems. It is a favorable approach due to the physicochemical and biocompatible properties of nanofibers, such as degradability, high surface area, and high porosity which can particularly accelerate the solubility of the drug in aqueous solutions and improve the efficacy of the drug [4]. Polymers used for fast-disintegrating oral drug delivery systems should be non-irritating and non-toxic, water soluble, disintegrate quickly upon contact with saliva, and have a good mouth feel. Both natural and synthetic polymers have been used to generate fast-disintegrating delivery systems [1,5,6]. Polysaccharides are used extensively for the development of biomaterials, as they are stable, non-toxic, biocompatible, and biodegradable [5,7]. In this study, the biopolymer pullulan has been used, a linear polysaccharide made from repeating maltotriose units linked by α-1,6 glycosidic units, with each maltotriose units comprised of three glucose units linked by α-1,4 glycosidic bonds. It is produced from the fungus *Aureobasidium pullulans,* and, unlike many other polysaccharides, is easily water soluble due to the low degree of hydrogen bonding [8,9]. Previous applications of electrospun systems of pullulan include drug transportation [10], filtration [11], medical scaffolds [12], food packaging with essential oils or antibacterial agents [13–17], and cosmetics [18]. Even, nanofibers of pullulan and pullulan/chitosan incorporated respectively with the drug molecule of rizatriptan [5] and aspirin [19] have been reported in purpose of fast-disintegrating drug delivery system.

To further increase the drug solubility, cyclodextrin inclusion complexes can be also incorporated into the nanofibers [20–23]. Cyclodextrins (CD) are a group of oligosaccharides composed of varying numbers of α-1,4-linked glucose units [24,25]. These form a cavity into which other compounds may enter and form an inclusion complex [24,25]. It has been shown the complexation between drug molecules and CDs increases the encapsulated compound's solubility and physicochemical properties [24,26,27]. The previous reports in which the inclusion complexes of cyclodextrins and different drug molecules including sulfisoxazole [28]; ciprofloxacin [29]; and naproxen [30] have been incorporated into electrospun nanofibers, have clearly demonstrated the enhanced dissolution and release profile of the given drugs. Hydroxypropyl-beta-cyclodextrin (HPβCD) is one of the most widely used modified CD types in pharmaceuticals, as it has been shown to have acceptable physicochemical properties and higher water solubility out of all natural CDs and their derivatives [24,25]. HPβCD has been studied extensively in animal and human trials and has been found to be well tolerated in animals and humans, particularly if taken orally [31]. As has been shown previously with various drug molecules, including antifungal [32,33], antibiotic [34], antiviral [26], anti-inflammatory [35], and steroid [36], encapsulation capability of HPβCD makes it a suitable means of increasing drug solubility in drug delivery systems.

Tetracycline is a commonly used antibiotic to treat a wide range of infections, such as typhus fever, Lyme disease, pneumonia, acne etc. To enhance its aqueous solubility and so bioavailability, hydrochloride form is being commonly used in oral dosage formulations. It has been reported that the hydrocholoride form of tetracycline can show two times higher water solubility in water compared to its basic form [37,38]. On the other hand, it has been shown that it is also possible to enhance the aqueous solubility and the release profile of tetracycline and/or its derivates by forming inclusion complexes with CDs [39–41]. Additionally, the incorporation of tetracycline into electrospun nanofibers has been reported previously for drug delivery purposes including the polymer systems of gelatin [42], chitosan [43], cellulose acetate [44], Eudragit [45], zein/polycaprolactone [46], dextran/polycaprolactone [47], polyvinyl alcohol/gum tragacanth [48], zein/gum tragacanth/poly lactic acid [49] and poly(ethylene-*co*-vinylacetate)/polylactic acid [50]. In these studies, the controlled/sustained release and/or the antibacterial activity of the tetracycline functionalized nanofibers have been examined to assert the potential to be used as drug delivery system. Even, in one of the related studies of Monteiro et al., polycaprolactone nanofibers has been functionalized with the inclusion complexes of βCD and tetracycline HCL where the controlled release and improved antibacterial property of tetracycline has been demonstrated [39]. In our study, we have early generated the electrospun nanofibers of pullulan which has been incorporated with the inclusion complexes of tetracycline-HPβCD to develop fast-disintegrating oral delivery system as an alternative to conventional tablet forms for drug dosage (Fig. 1).

2. Experimental procedures

2.1. Materials

Hydroxypropyl-beta-cyclodextrin (HPβCD, Cavasol W7, DS: ~0.9) was gifted by Wacker Chemie AG (USA). The as-received pullulan (Mw: 300,000 g/mol, TCI America), tetracycline (>98%, Sigma-Aldrich), dimethyl sulfoxide (DMSO, >99.9%, Sigma-Aldrich), buffer chemicals (phosphate buffered saline tablet (Sigma Aldrich), sodium phosphate dibasic heptahydrate (Na_2HPO_4, 98.0–102.0%, Fisher Chemical), potassium phosphate monobasic (KH_2PO_4, ≥99.0%, Fisher Chemical), sodium chloride (NaCl, >99%, Sigma Aldrich), o-phosphoric acid (85% (HPLC), Fisher Chemical)) were provided commercially. The required water was distilled by Millipore Milli-Q ultrapure water system (Millipore, USA).

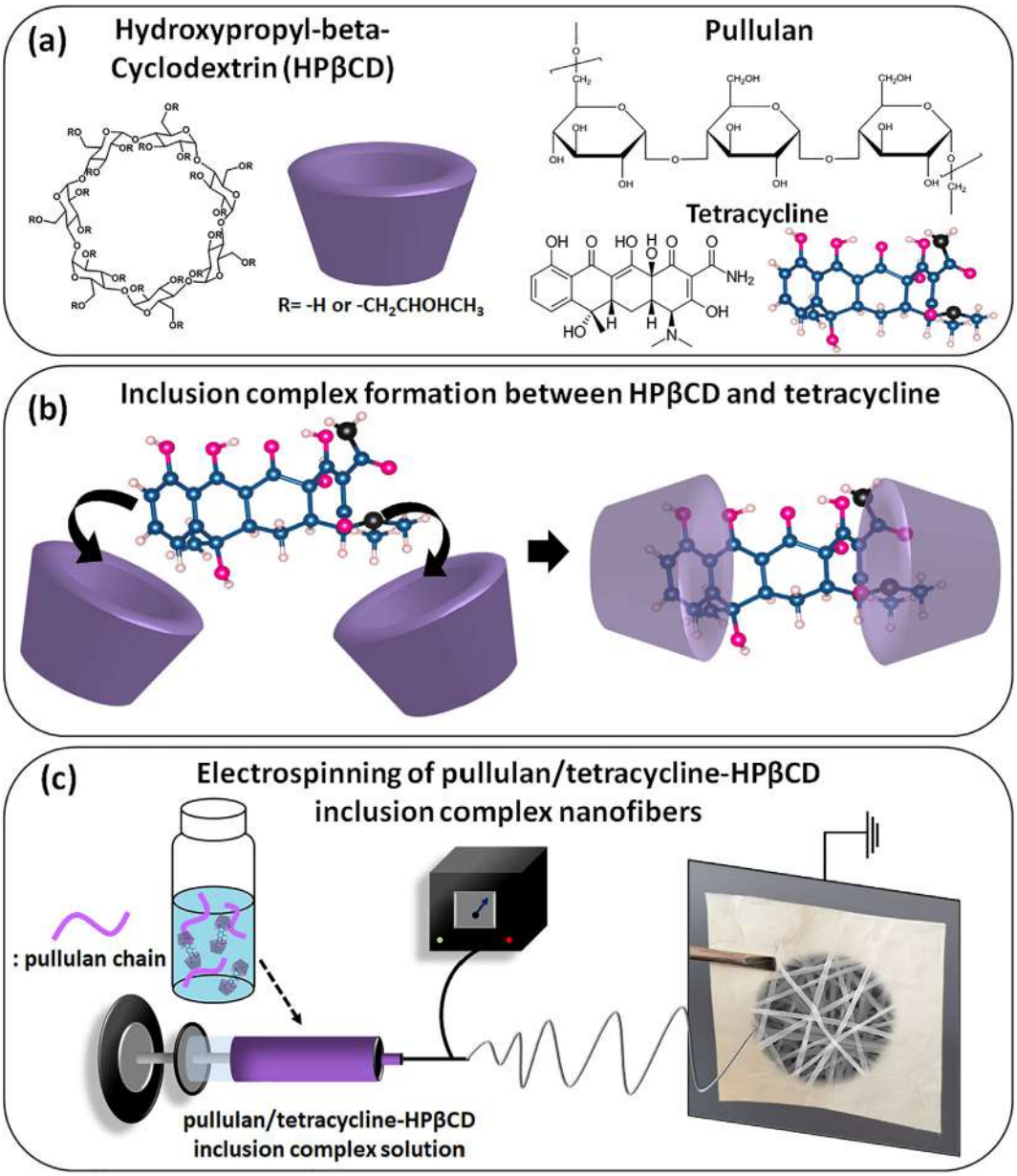

Fig. 1. (a) The chemical structure of HPβCD, pullulan and tetracycline. (b) The schematic representation of inclusion complex formation between HPβCD and tetracycline and (c) the electrospinning of pullulan/tetracycline-HPβCD-inclusion complex (IC) nanofibers.

2.2. Modeling studies

The quantum mechanical calculations based on density functional theory (DFT) [51,52] were carried out by using Vienna ab initio Simulation Package (VASP) [53]. The exchange–correlation functional was described by generalized gradient approximation (GGA-PBE) [54] including van der Waals corrections (DFT-D2) [55]. The pseudopotentials of elements (C, O, H, and N) were represented by the projector augmented-wave (PAW) approach [56]. The plane-wave basis set with a kinetic energy cutoff of 520 eV was used for all calculations. All the structures were relaxed by using a conjugate gradient algorithm until the force on each ion was less than10 meV, and the total energy difference between sequential self-consistent electronic steps were smaller than 10^{-5} eV. The integrations over the Brillouin zone were computed at the Γ-point. The effect of solvent was taken into account with an implicit solvation model [57].

2.3. Phase solubility

To determine the phase solubility profile of tetracycline, excess amount of drug was mixed with increasing concentrations of HPβCD, ranging from 0 to 64 mM, in 5 mL of water. It was shaken on an orbital shaker at 450 rpm at room temperature shielded away from light. After 24 h, the solutions were filtered using a 0.20 μm PTFE filter, and the UV–vis spectroscopy (PerkinElmer, Lambda 35, USA) was used to measure the absorbance intensity of the filtered aliquots (275 nm). The experiment was repeated three times to obtain an average ± standard deviation. The calibration curve ($R^2 \geq 0.99$) of tetracycline in water was used to plot the phase solubility diagram. Additionally, the binding constant (K_S) was calculated by using the following equation (Eq. (1)).

$$Ks = slope/S_0(1\text{-}slope) \quad (1)$$

where slope belongs to linear part of the diagram and S_0 is the intrinsic solubility of tetracycline (~0.9 mM).

2.4. Electrospinning

Firstly, the inclusion complexes (IC) of tetracycline with HPβCD were prepared in a 1:2 (drug:HPβCD) mole ratio that corresponds to the ~ 7.7 % (w/w) drug content in the sample. For this, the HPβCD (20%, w/v) were dissolved in distilled water, and the drug were added to the solution and stirred overnight at room temperature. Pullulan was added to the tetracycline-HPβCD-IC system (15%, w/v) and stirred at room temperature until the polymer dissolved completely. Control samples of pure pullulan, pullulan/HPβCD and pullulan/tetracycline were prepared, as well. For pristine pullulan sample, 20% (w/v) polymer concentration was used while other samples were contained 15% (w/v) of pullulan. The pullulan/tetracycline nanofibers were incorporated with the same ratio of drug to total sample (w/w) as in the sample with inclusion complexes (~7.7 %). The solutions' conductivity and viscosity were measured before electrospinning. To measure the conductivity, a conductivity-meter was used (FiveEasy, Mettler Toledo, USA) at room temperature. The viscosity of solutions was measured using a rheometer (AR 2000 rheometer, TA Instrument, USA) with a 20 mm, 4° cone-plate spindle, at a shear rate of 0.01 to 1000 s^{-1} at 20 °C. Here, viscosities of samples were compared according to arithmetic mean value calculated from the shear rate range of ~ 200–900 s^{-1}. For electrospinning, each solution was individually loaded into 1 mL syringes with a 27 G needle and placed horizontally on the syringe pump of electrospinning equipment (Spingenix, model: SG100, Palo Alto, USA) in a 20 °C and 22% relative humidity environment. A high voltage of 15 kV was supplied to the stainless-steel needle at the same time that the electrospinning solution was pushed through the syringe at a steady rate of 0.7 mL/h. The nanofibers were deposited on a metal collector plate covered with aluminum foil 15 cm away from the syringe.

2.5. Morphology analysis

The scanning electron microscope (SEM, Tescan MIRA3, Czech Republic) images of pullulan/tetracycline-HPβCD-IC and pullulan/tetracycline, pullulan/HPβCD, and pristine pullulan nanofibers were obtained to analyze sample morphology. The average fiber diameter and standard deviations of ~ 100 nanofibers were calculated using the SEM images and ImageJ software.

2.6. Fourier transform infrared spectroscopy

The Fourier transform infrared (FTIR) spectra (ATR-FTIR spectrometer, PerkinElmer, USA) were obtained for tetracycline powder, HPβCD powder, and all nanofibers that were generated. The FTIR graphs were recorded from 4000 – 600 cm^{-1} at a resolution of 4 cm^{-1} for 32 scans.

2.7. X-ray diffraction

X-ray diffractometry (XRD, Bruker D8 Advance ECO, USA) was used to determine the X-ray diffraction patterns of tetracycline powder, HPβCD powder, and all nanofibers-based samples. The XRD scanning was performed from 2θ of 8° to 30° using Cu-Kα source.

2.8. Thermal characterization

Thermal profiles of tetracycline powder, HPβCD powder, and nanofibers were obtained using thermogravimetric analysis (TGA, Q500, TA Instruments, USA) and differential scanning calorimetry (DSC, Q2000, TA Instruments, USA). For TGA, the samples were heated in a platinum pan at a rate of 20 °C/min from 30 °C to 600 °C under inert environment (N_2). For DSC, the samples were weighed and placed in a Tzero aluminum pan and heated at a rate of 10 °C/min from 0 °C to 180° using inert purging gas (N_2).

2.9. Loading efficiency

To calculate the loading efficiency of samples, a fixed amount of pullulan/tetracycline-HPβCD-IC and pullulan/tetracycline nanofibers (1 mg) were dissolved in DMSO (3 mL). The tetracycline content in these samples were measured using UV–vis spectroscopy (292 nm), and a calibration curve of tetracycline in DMSO was taken with linearity and acceptability of $R^2 \geq 0.99$. The loading efficiency percentage was calculated using the following equation (Eq. (2)).

$$\text{Loading efficiency (\%)} = Ce/Ct \times 100 \quad (2)$$

where Ce is the concentration of loaded tetracycline and Ct the initial concentration of tetracycline in the nanofibrous samples. The results were repeated three times to obtain an average ± standard deviation (n = 3).

2.10. Dissolution test

The dissolution of the nanofibers of pullulan/tetracycline-HPβCD-IC and pullulan/tetracycline were measured using UV–vis spectroscopy. For this, ~10 mg of each sample was dissolved in 5 mL of PBS buffer (pH 7.4) using an orbital shaker at 200 rpm at room temperature for 10 min, and then the samples were filtered using a PTFE filter (0.45 μm) prior the measurements. The experiments were repeated three times to obtain an average ± standard deviation (n = 3).

2.11. Time dependent in-vitro release test

To determine the release of tetracycline from the nanofibers, the same amount of pullulan/tetracycline-HPβCD-IC and pullulan/tetracycline-based samples (~10 mg) were immersed in 10 mL of PBS buffer solution (pH 7.4). The samples were shaken on an orbital shaker at 200 rpm at room temperature. Aliquots of 1 mL were removed from each sample and replaced with 1 mL of fresh PBS buffer at set time intervals. The UV–vis spectra were recorded (272 nm) for the repeated experiments (n = 3). The release kinetic of each sample was studied using different kinetic models (see supporting information).

2.12. Disintegration test

The disintegration profiles of pullulan/tetracycline-HPβCD-IC and pullulan/tetracycline nanofibers were followed in an artificial saliva environment (pH 6.8) to simulate disintegration in the oral cavity [58]. For this, filter paper was placed in petri dishes (10 cm) and wetted with 10 mL of the artificial saliva solution (2.38 g Na_2HPO_4, 0.190 g KH_2PO_4, 8 g NaCl in 1L distilled water and adjusting of pH to 6.8 with phosphoric acid). The excessed solution was drained and nanofiber samples of dimensions ~ 2.5 cm by 3.0 cm (~10 mg) were placed individually on the wetted filter papers. Simultaneously, a video was filmed during the disintegration of the nanofibers (Video S1).

2.13. Antibacterial test

The antibacterial performance of pullulan/tetracycline-HPβCD-IC, pullulan/tetracycline and pullulan/HPβCD nanofibers were

tested against *Escherichia coli* (*E. coli*) (BL21 (NEB)) and *Staphylococcus aureus* (*S. aureus*) (ATCC 25923) by disk-diffusion assay. These strains were streaked on LB-agar plates and grown overnight at 37 °C. Colonies were dissolved in sterile 1X PBS to a McFarland standard of ~ 0.5. Sterile cotton swabs were then used to spread them on LB-agar plates. Samples were cut into circular pieces with ~ 15 mm diameter having identical weight (~12 mg). As a positive control, 20 ul of tetracycline (20 mg/ml) was added to filter papers having the same diameter with nanofibers (~15 mm). Three pieces of each sample were placed on agar plate separately and plates were incubated in 37° C incubator for ~ 24 h (n = 3). Photos of the bacterial growth on plates were acquired in BioRad ChemiDoc Image Acquisition system and zones of inhibition were calculated from these photos.

2.14. Statistical analysis

The statistical analyses were conducted by using the one-way/two-way of variance (ANOVA). OriginLab (Origin 2021b, USA) was used for all these ANOVA analyses (0.05 level of probability).

3. Results and discussion

3.1. Phase solubility analysis

The effect of increasing concentrations of HPβCD on the solubility of tetracycline molecules has been determined through phase solubility analysis, as it has been shown that CD can increase the drug solubility [27]. Here, the phase solubility diagram has been plotted from 0 to 64 mM of HPβCD and has showed negative deviation from linearity (i.e. A_N-type profile according to Higuchi and Connors) which suggests the decreasing effect of solubilizer by its increasing concentration (Fig. 2) [27,59]. The intrinsic solubility of tetracycline in water is ~ 0.9 mM and has increased by a factor of ~ 2.1 at the highest HPβCD concentration (64 mM) due to inclusion complexation. On the other hand, the binding constant K_s for the tetracycline-HPβCD system has been found to be 21 M^{-1}. In one of the related studies, Moreno-Cerezo et al. has found the same diagram profile of A_N for tetracycline-HPβCD system [41]. However, the binding constant has been reported as 119 M^{-1} and this might be originated from using the HCL derivatives of tetracycline.

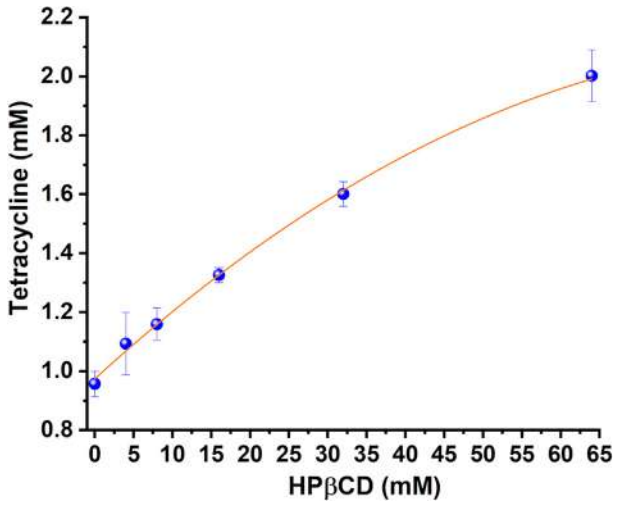

Fig. 2. Phase solubility diagram of tetracycline against increasing HPβCD concentrations.

3.2. Molecular modeling analysis

The inclusion complex formation between tetracycline and HPβCD has been further examined with *ab initio* computational methods. Firstly, all structures have been optimized to determine the ground state geometries of quest molecule and host CD both in vacuum and water. Next, the interaction between tetracycline and HPβCD has been examined as a function of distance for various possible configurations initially in a vacuum. In this respect, head (H) - tail (T) orientation of tetracycline and narrow (A) – wide (B) rim orientation of HPβCD are considered. For 1:1 (tetracycline: HPβCD) stoichiometry, tetracycline has penetrated through the wide rim, and inclusion complex could be formed for both head and tail orientations. The lowest energy configuration has been shown in Fig. 3a. The strength of binding between the quest molecule and host CD can be quantified by complexation energy (E_{CE}), which has been obtained by the following equation (Eq. (3)).

$$E_{CE} = n^{*}E_T[HP\beta CD] + E_T[\text{tetracycline}] - E_T[\text{tetracycline: } HP\beta\text{CD-IC}] \quad (3)$$

where E_T[HPβCD], E_T[tetracycline], and E_T(tetracycline:HPβCD-IC) are the total energies of HPβCD, tetracycline, and tetracycline: HPβCD inclusion complex (IC), respectively. All the energies have been computed both in a vacuum and in the solvent. In our system, n is equal to 1 for 1:1 and 2 for 1:2 M ratio. As listed in Table 1, E_{CE} for head orientation (AB-H) has been significantly larger than tail orientation (AB-T) correlated to size match. Additionally, high E_{CE} has indicated that the interaction between tetracycline and HPβCD is strong, and IC formation is energetically favorable. Similar trends have been obtained when the calculations have been repeated in water, but the reduction in binding strength (i.e., reduced E_{CE}) between tetracycline and HPβCD has been noticed. Following the 1:1 case, 1:2 stoichiometry has been also examined. Two possible configurations have been obtained for IC formation, and the most favorable one has been shown in Fig. 3b. In this configuration, two HPβCD's have been oriented so that tetracycline has penetrated through the wider rims. As reported in Table 1, E_{CE} significantly has increased for 1:2 M ratio, suggesting it as a more favorable stoichiometry for tetracycline:HPβCD-IC. In addition to complexation energies, the solvation energy (E_{SE}), which can provide insight into solubility, has been investigated. E_{SE} can be estimated by considering the following relation.

$$E_{SE} = E_T{}^{water}[\text{tetracycline:HP}\beta\text{CD-IC}] - E_T{}^{vacuum}[\text{tetracycline:HP}\beta\text{CD-IC}] \quad (4)$$

where E_T^{water}[tetracycline:HPβCD-IC] and E_T^{vacuum}[tetracycline: HPβCD-IC] are the total energies of IC calculated in water and vacuum, respectively. E_{SE} has been obtained only for the most favorable configurations and given in Table 1. Upon complex formation, E_{SE} of tetracycline (-27.60 kcal/mol) significantly has increased and become −73.89 and −130.93 kcal/mol for 1:1 and 1:2 stoichiometry, respectively. The noticeable increase in E_{SE} following the complex formation has indicated an enhancement in solubility of tetracycline.

3.3. Morphology characterization

As it has been also discussed in the molecular modeling section, 2:1 (CD:drug) molar ratio is more favorable compared to 1:1 one. It has been also found that 2:1 M ratio resulted in a stable system fit for electrospinning and formation of nanofibers. Here, the concentration of 15% (w/v) and 20% (w/v) has been used for pullulan and HPβCD, respectively. For the control samples, the amount of drug was equal to the percentage (~7.7 %, w/w) in inclusion complex-based system. The solution properties of viscosity and conductivity

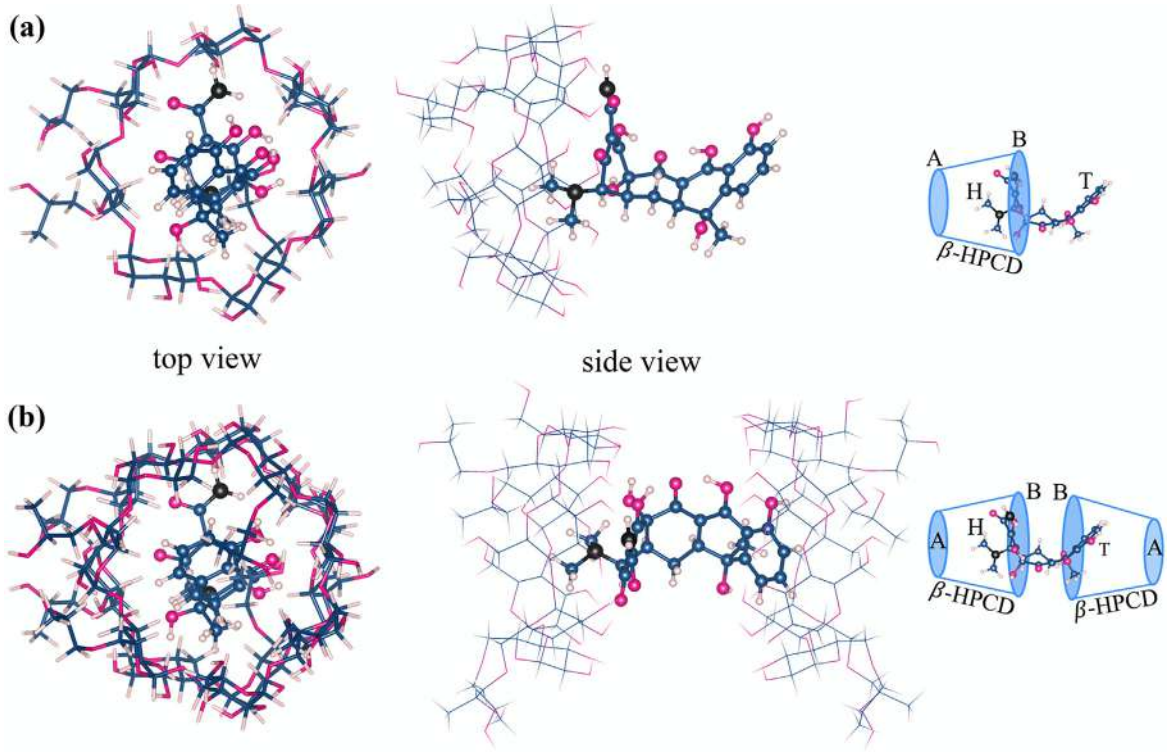

Fig. 3. The top and side view of tetracycline:HPβCD-IC for (a) 1:1 and (b) 1:2 stoichiometry. The orientation of tetracycline (head-H, and tail-T) and HPβCD (narrow rim-A and wide rim-B) is labeled.

Table 1
The complexation and solvation energies of tetracycline:HPβCD-IC for different orientations in 1:1 and 1:2 stoichiometry.

Guest:Host	Molar Ratio	Orientation	E_{CE} (vacuum) kcal/mol	E_{CE} (water) kcal/mol	E_{SE} kcal/mol
Tetracycline:HPβCD	1:1	AB-H	31.55	12.14	−73.89
	1:1	AB-T	11.38	–	–
	1:2	AB-HT-AB	30.42	–	–
	1:2	ABBA	43.61	15.55	−130.93

Table 2
The solution properties and fiber diameters of resulting electrospun nanofibers.

Sample	Pullulan conc. (%, w/v)[a]	HPβCD conc. (%, w/v)[a]	Drug conc. (%, w/w)[b]	Viscosity (Pa·s)	Conductivity (μS/cm)	Average fiber diameter (nm)
pullulan	20	–	–	0.489	38.3	590 ± 95
pullulan/HPβCD	15	20	–	0.296	123.8	705 ± 155
pullulan/tetracycline-HPβCD-IC	15	20	7.7	0.399	172.5	640 ± 125
pullulan/tetracycline	15	20	7.7	0.369	71.5	290 ± 65

[a]with respect to solvent (water); [b]with respect to total sample amount.

have been summarized in Table 2 along with the average fiber diameter of each sample. In general, the addition of both HPβCD and tetracycline has resulted in an increase in the conductivity value of solutions. Here, pullulan/tetracycline-HPβCD-IC nanofibers have shown thinner fiber diameter (640 ± 125 nm) compared to pullulan/HPβCD nanofibers (705 ± 155 nm). The pullulan/tetracycline-HPβCD-IC solution has indicated a higher viscosity compared to pullulan/HPβCD solution, however, the difference in viscosities have been less significant than the difference in conductivities. Therefore, electrified jet of pullulan/tetracycline-HPβCD-IC solution having higher conductivity value has been stretched out more during the electrospinning process to create thinner fibers [60]. When comparing the pullulan and the pullulan/tetracycline fibers, the addition of tetracycline has not only increased the conductivity but also has decreased the viscosity. The result is that there has been a significantly lower average fiber diameter for the pullulan/tetracycline nanofibers (290 ± 65 nm) compared to pullulan nanofibers (590 ± 95 nm) (Table 2). This data correlates with previous data from the literature that has demonstrated that higher conductivity and lower viscosity result in thinner nanofibers due to higher stretching effect on the electrospinning jet during the process [36,60]. The statistical analyses have revealed that the means values of nanofibers are significantly different from each other's ($p < 0.05$)).

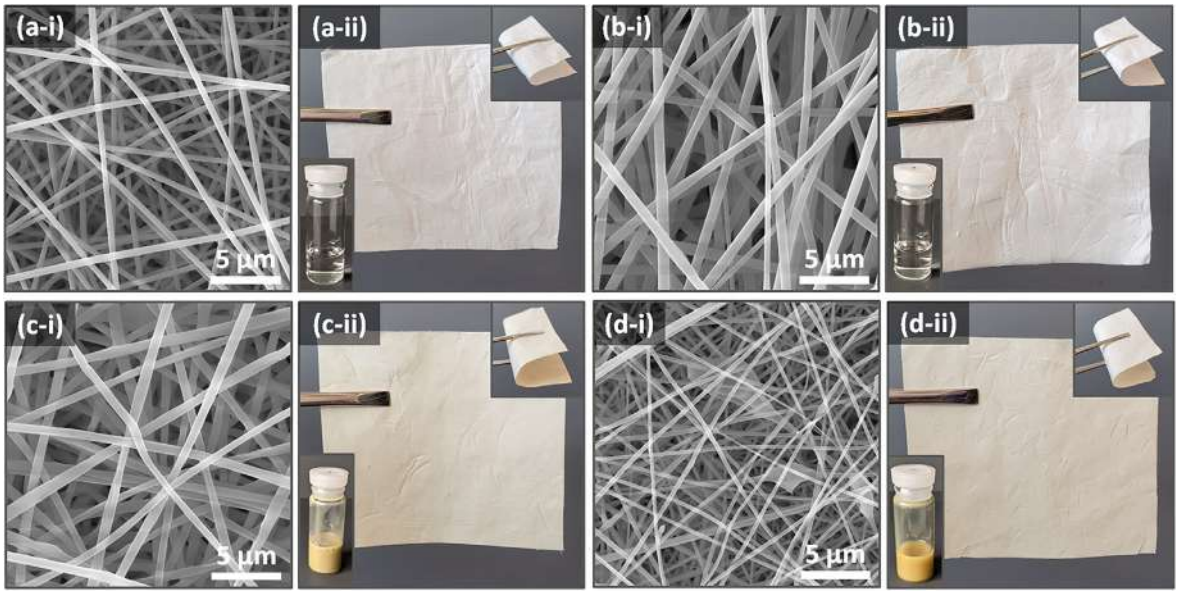

Fig. 4. (i) SEM images and (ii) photos of electrospinning solutions, and electrospun nanofibers of (a) pullulan, (b) pullulan/HPβCD, (c) pullulan/tetracycline-HPβCD-IC, (d) pullulan/tetracycline.

The scanning electron microscopy (SEM) images seen in Fig. 4 have showed that the systems of pullulan, pullulan/HPβCD, pullulan/tetracycline-HPβCD- IC and pullulan/tetracycline, all yielded defect -free nanofibers, which were free-standing and flexible. It is noteworthy that the solution of pullulan/tetracycline-HPβCD-IC (Fig. 4c-ii) has been lighter in color than the control sample of pullulan/tetracycline (Fig. 4d-ii). Pure tetracycline powder has a dark yellow color; as CD have been shown to have color-masking capabilities; the lighter color of pullulan/tetracycline-HPβCD-IC might be an indication of inclusion complex formation between HPβCD and tetracycline [24,61]. In Fig. 4d-i, it is obvious that the pullulan/tetracycline nanofibers have had crystals on the fibers, indicating the drug has not been incorporated into the fiber homogenously. In comparison, Fig. 4c-i has indicated that drug crystals have not been detected in the pullulan/tetracycline-HPβCD-IC nanofibers. This may support the inclusion complex formation which has allowed tetracycline to distribute throughout the fiber in an amorphous and homogeneous manner.

3.4. Structural characterization

The structural analyses of samples have been conducted using Fourier transform infrared (FTIR) spectroscopy (Fig. 5). In case of HPβCD, peaks at 3324–3355 cm^{-1}, 2930 cm^{-1}, 1650 cm^{-1} and 1370 cm^{-1} correspond to –OH stretching, C—H stretching, O—H bending and $-CH_3$ bending, respectively. The absorption bands at 1028 cm^{-1}, 1150 cm^{-1} and 1180 cm^{-1} correspond to coupled C—C/C—O stretching and antisymmetric C—O—C glycosidic bridge stretching [62,63]. The FTIR spectra of pristine pullulan and HPβCD have been detected analogous in the parallel region of the spectrum due to the similar structures of the glucose and glucopyranose units that form their chemical compositions. Pristine pullulan nanofibers have also exhibited absorption peaks located at 3313 cm^{-1}, 2925 cm^{-1}, and 1641 cm^{-1}, corresponding to the ν(O—H) stretching, ν(C—H) stretching and H—O—H bending, respectively, and intense peaks from 1200 cm^{-1} and 1000 cm^{-1} are due to the ν(C—O) stretching [7,17,64]. For the FTIR spectrum of tetracycline, distinct absorption bands have been found at ~ 1578 cm^{-1} and ~ 1222 cm^{-1}, corresponding with C=C stretching peaks and aromatic in-plane deformation peaks, respectively [65]. In the FTIR spectrum of pullulan/tetracycline-HPβCD-IC nanofibers, in addition to the peaks from pullulan and HPβCD, peaks at ~ 1610 cm^{-1} and ~ 1232 cm^{-1} have been detected (Fig. 5b). The respective peaks corresponds to the characteristic peaks from tetracycline, and the shift to a higher wavenumber has been an indicative of interactions between tetracycline and HPβCD by inclusion complexation [36,62]. The same characteristic peaks have been detected at a very low intensity without a shift in the spectrum of pullulan/tetracycline nanofibers demonstrating the physical mixture of pullulan and tetracycline in the absence of specific interaction (Fig. 5b).

X-ray diffractometry (XRD) has been also performed to examine the crystalline structure of samples. Fig. 6a shows the XRD pattern of the powder form of the tetracycline and HPβCD, and the nanofiber samples. Here, tetracycline has showed peaks at $2\theta \approx 9.1$, 11.8, and 17.8 due to its crystal nature [39]. On the other hand, HPβCD powder, pullulan nanofibers and pullulan/HPβCD nanofibers have shown broad halos in the XRD graphs suggesting their amorphous structure [7,36]. The characteristic peaks of tetracycline have been observed in case of pullulan/tetracycline nanofibers at low intensities (Fig. 6a). In contrast, the XRD graph of pullulan/tetracycline-HPβCD-IC nanofibers have not showed any characteristic peaks corresponding with tetracycline's crystalline structure, indicating that inclusion complexation with HPβCD has allowed tetracycline to take on an amorphous distribution within the fibers [36,39].

In differential scanning calorimetry (DSC) thermogram of tetracycline, Fig. 6b, there has been an endothermic peak at 160 °C that represented the melting point temperature. It has been known that inclusion complexation with CD can cause reduction or absence of endothermic peaks of the drug molecule at its melting point [66]. The DSC thermogram for pullulan/tetracycline-HPβCD-IC nanofibers have not indicated an endothermic peak at 160 °C, meaning the tetracycline incorporated into the nanofiber no longer has a crystalline structure. This has corresponded with the amorphous distribution found in the XRD graph of tetracycline. The DSC thermogram of pullulan/tetracycline nanofibers have had a very slight divot at 160 °C, which may be a result of crystalline tetracycline present in the nanofiber (Fig. S1). This divot has been detected to

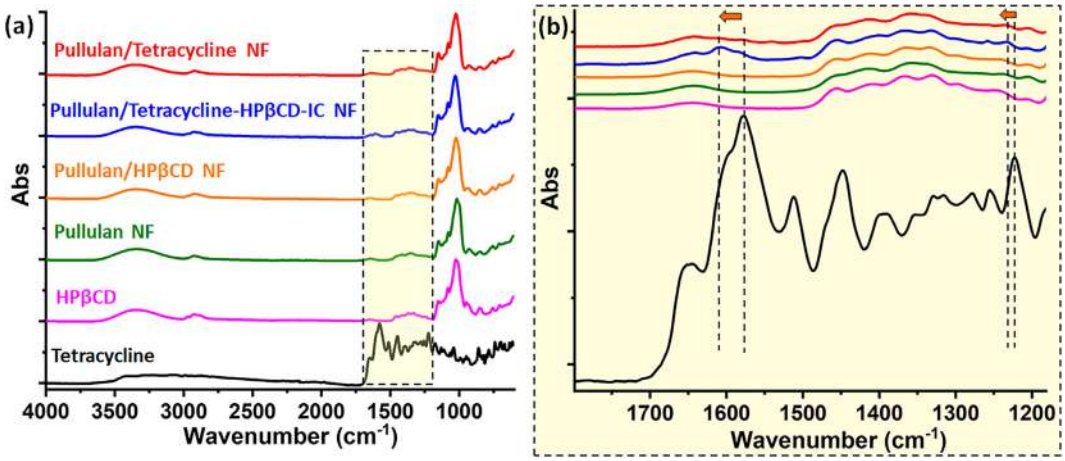

Fig. 5. (a) The full and (b) the expanded range FTIR spectra of tetracycline, HPβCD powder, pullulan nanofibers (NF), pullulan/HPβCD NF, pullulan/tetracycline-HPβCD-IC NF, and pullulan/tetracycline NF.

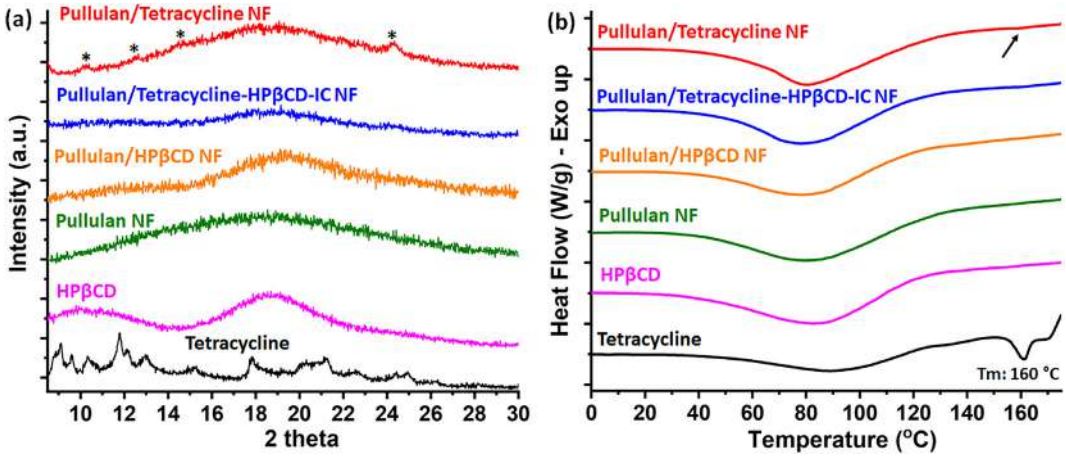

Fig. 6. (a) XRD graphs and (b) DSC thermograms of tetracycline, HPβCD powder, pullulan nanofibers (NF), pullulan/HPβCD NF, pullulan/tetracycline-HPβCD-IC NF, and pullulan/tetracycline NF.

be a slight one since the melting peak of pure tetracycline does not have a sharp and distinct profile. On the other hand, the broad endothermic peak observed at around 90 °C for all samples has been originated from the dehydration of water content [13,36].

The thermal degradation profile of samples has been examined using thermogravimetric analyzer (TGA) (Fig. 7). TGA thermograms of pullulan and pullulan/HPβCD nanofibers have showed two weight losses; the weight loss up to 100 °C was due to evaporation of water from the sample, and the second weight losses at 327 °C and 350 °C corresponded to the main degradation of pullulan and pullulan/HPβCD systems, respectively. On the other hand, tetracycline has showed the main degradation at around 190 °C. It is clear in the derivative thermograms (DTG) that there has been a shift to the higher temperature range and broadening by the incorporation of HPβCD into the pullulan nanofibers (Fig. 7a-ii, b-ii). It is also obvious in Fig. 7a-ii, the DTG of pullulan/tetracycline-HPβCD-IC nanofibers has resulted in a shift to a lower degradation temperature of pullulan/HPβCD one and has become sharper compared to DTG of pullulan/HPβCD nanofibers. In comparison, the DTG of pullulan/tetracycline nanofibers have not resulted in a significant profile change compared to the pure pullulan nanofibers. The change in the DTG profile of pullulan/tetracycline-HPβCD-IC nanofibers might support the inclusion complex formation within the system. In contrast, the DTG for pullulan/tetracycline nanofiber has merely decreased which indicating incorporation of the drug into the nanofiber without further interaction [26].

3.5. Pharmacotechnical properties

The loading efficiency of the fibers has been determined by dissolving samples in DMSO. It has been found that the pullulan/tetracycline-HPβCD-IC nanofibers and the pullulan/tetracycline nanofibers have had loading efficiencies of 100.2 ± 0.8 % and 100.5 ± 6.4 %, respectively. These relatively similar values show that there has been no loss of drug molecules during the preparation of the samples or during the electrospinning process. In another word, the ultimate nanofibers of pullulan/tetracycline-HPβCD-IC and pullulan/tetracycline have been obtained having the initial molar ratio of 2:1 (CD:drug) and so initial drug content of ~ 7.7 % (w/w).

The dissolutions of tetracycline in nanofibers with and without HPβCD has been found using UV–vis spectroscopy and have been given in Fig. 8a. The absorption of tetracycline has been detected to be higher when inclusion complex system has presented within the nanofibers. The finding has indicated that the pullulan/tetracycline-HPβCD-IC nanofibers have had an average absorption 1.36 ± 0.04 times higher than pullulan/tetracycline nanofibers. This has correlated with higher solubility of tetracycline due to inclusion complex formation with HPβCD.

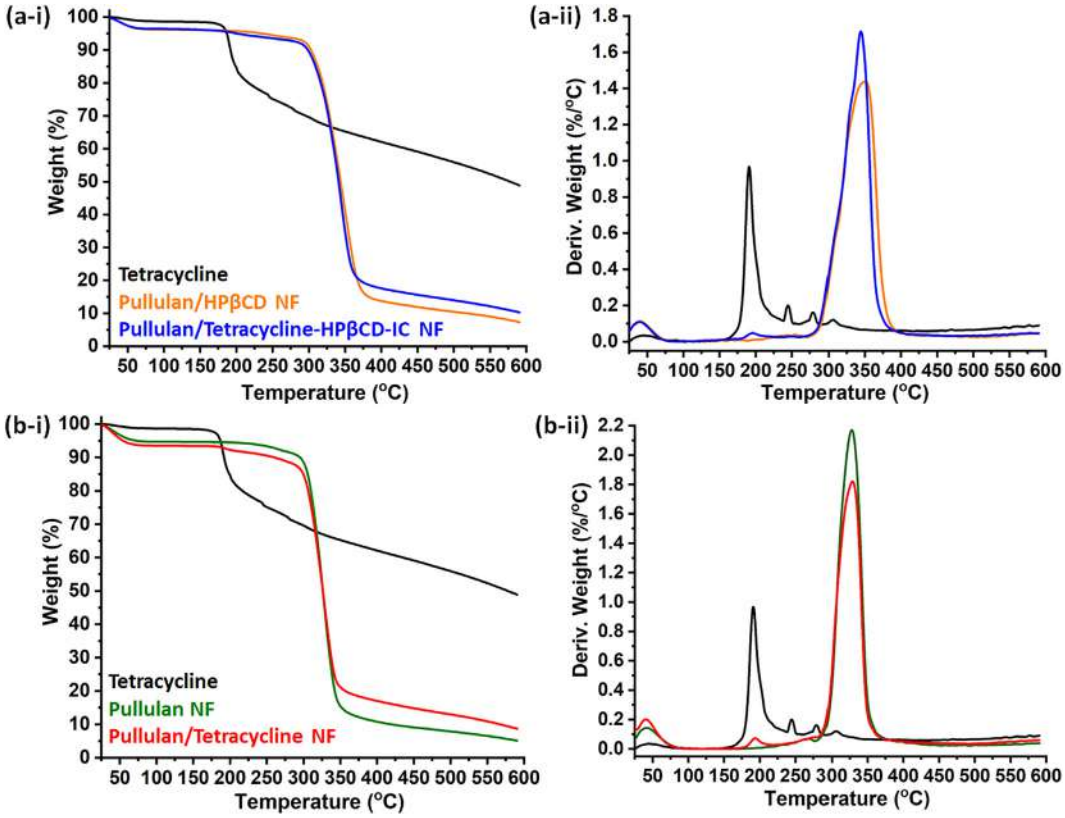

Fig. 7. (i) TGA thermograms and (ii) the derivative graphs (DTG) of (a) tetracycline, pullulan/HPβCD nanofibers (NF), and pullulan/tetracycline-HPβCD-IC NF, (b) tetracycline, pullulan NF, and pullulan/tetracycline NF.

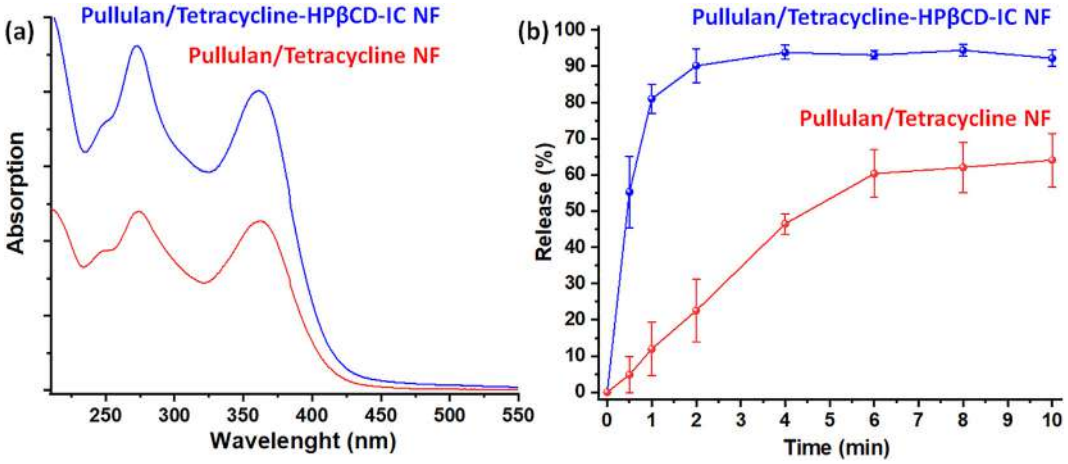

Fig. 8. (a) Representative UV–vis graph of pullulan/tetracycline-HPβCD-IC nanofibers (NF) and pullulan/tetracycline NF. (b) Time-dependent *in-vitro* release profile of pullulan/tetracycline-HPβCD-IC NF and pullulan/tetracycline NF.

The time dependent *in-vitro* release profiles of pullulan/tetracycline-HPβCD-IC nanofibers and pullulan/tetracycline nanofibers have been given in Fig. 8b. Pullulan/tetracycline-HPβCD-IC nanofibers has released ~ 55% of tetracycline just in 30 s. It has reached the maximum release percentage of ~ 94 % in two minutes and has showed steady release profile up to 10 min. On the other hand, pullulan/tetracycline nanofibers have reached its maximum release percentage (65%) in 8–10 min. It is evident that due to inclusion complex formation with HPβCD, tetracycline has been released in a higher and faster manner in case of pullulan/tetracycline-HPβCD-IC nanofibers compared to the control sample of pullulan/tetracycline nanofibers. For pullulan/tetracycline-HPβCD-IC nanofibers, the solid content ratio of pullulan:CD is 1:1 (20 % w/v for each) and HPβCD has a significantly higher water solubility (>2000 mg/mL) compared to pullulan polymer (~500 mg/mL). In addition to enhanced dissolution of tetracycline, higher aqueous solubility might have been provided in case of pullulan/tetracycline-HPβCD-IC nanofibers than pullulan/tetracycline nanofibers and this might have contributed to the better release profile of inclusion complex incorporated sample. Briefly, the release of tetracycline from pullulan/tetracycline nanofibers has occurred by the steady dissolution of tetracycline crystals in the aqueous medium, while

the inclusion complex structure of tetracycline-HPβCD has ensured the faster dissolution of pullulan/tetracycline-HPβCD-IC nanofibers. Additionally, the statistical analyses have showed the significant variations between samples ($p < 0.05$).

The release profiles of electrospun nanofibers have been also evaluated by different kinetic models. The formulations and correlation coefficient values (R^2) (Table S1) have been given in supporting information. The results have showed that the release profile of pullulan/tetracycline-HPβCD-IC nanofibers has not fitted to zero/-first order and Higuchi models (Table S1). This result has suggested that tetracycline has not released with a time dependent manner from a water insoluble planar matrix in case of pullulan/tetracycline-HPβCD-IC nanofibers (Fick's first law) [67]. On the other hand, a relatively higher R^2 value (0.8297) has been detected for the kinetic model of Korsmeyer–Peppas compared to other kinetic models and the diffusion exponent (n) value (0.6836) has been determined in the range of $0.45 < n < 0.89$. This might be due to the irregular/non-Fickian diffusion and erosion-controlled release of tetracycline from pullulan/tetracycline-HPβCD-IC nanofibers [67,68]. In contrast, pullulan/tetracycline nanofibers have displayed higher R^2 (>0.9000) values for each of respective kinetic models than pullulan/tetracycline-HPβCD-IC nanofibers (Table S1). This has supported that the release of tetracycline from pullulan/tetracycline nanofibers has occurred both in a time-dependent and diffusion/erosion-controlled manner [67,68].

The disintegration profiles of the nanofibers have been evaluated in an artificial saliva environment created with filter paper (Fig. 9, Video S1). Here, pullulan/tetracycline-HPβCD-IC nanofibers have been absorbed by the wetted filter paper and have completely disintegrated in this simulated environment within two seconds (Fig. 9a). However, a thin layer has been left as residue on the surface of the filter paper in case of pullulan/tetracycline nanofibers (Fig. 9b). This might be originated from the content of crystalline drug molecules in the nanofibers and lower aqueous solubility of absolute pullulan compared to HPβCD included nanofiber. The darker color observed of pullulan/tetracycline-HPβCD-IC nanofibers on the wetted filter paper compared to pullulan/tetracycline nanofibers might be also due to the efficient absorption of inclusion complex based system. Briefly, pullulan/tetracycline-HPβCD-IC nanofibers would be more suitable for an oral fast-disintegrating delivery system, as it would disintegrate quickly and without leaving a grainy feeling behind upon administration.

3.6. Antibacterial performance

The antibacterial activity of samples has been explored by disk-diffusion assay against Gram positive (*S. aureus*) and Gram negative (*E. coli*) bacteria. Fig. 10 has indicated the photos of plates and Table 3 has summarized the calculated diameter of inhibition zones from photos. As a positive control the filter paper having the same diameter (∼15 mm) as the nanofibers have been spotted with the stock solution of tetracycline. Since, filter paper is not soluble in the agar medium, it has also indicated the exact sample size used for the nanofibrous samples. Due to antibacterial property of tetracycline, the positive controls have showed transparent circles for both *S. aureus* and *E. coli* owing to inhibition of bacterial growth in the given area (Fig. 10a-i,ii) [69]. As it is observed, tetracycline has demonstrated better antibacterial activity against *E. coli* (49.86 ± 0.81) compared to *S. aureus* (28.10 ± 0.46). The statistical analyses have also showed the significant variations between bacteria strain types ($p < 0.05$). Although it is known that a broad-spectrum antibiotic such as tetracycline exhibits similar bactericidal activity on both a wide range of gram-positive and -negative organisms like *S. aureus* and *E. coli*, these relative differences in antibacterial activity may be attributed to differential permeation patterns from the cell-membranes or relative uptake from receptors in each class of organism [70,71]. As is expected, the control sample of pullulan/HPβCD nanofibers has not exhibited an antibacterial property (Fig. 10b-i,ii). On the other hand, pullulan/tetracycline-HPβCD-IC nanofibers have demonstrated an antibacterial activity with the external inhibition zone diameter of 48.91 ± 0.23 mm and 28.91 ± 0.46 mm for *E. coli* and *S. aureus,* respectively (Table 3 and Fig. 10d-i,ii). The statistical analyses have revealed that there has been a non-significant difference between pullulan/tetracycline-HPβCD-IC and pullulan/tetracycline nanofibers with $p = 0.13$ value. However, slightly wider inhibition zones for pullulan/tetracycline-HPβCD-IC nanofibers have shown the moderately better antibacterial activity of this sample compared to pullulan/tetracycline one (Table 3). This might be due to the enhanced solubility of tetracycline by inclusion complexation which has provided a better penetration of drug molecules through the agar medium. It has been also noted that, both nanofibrous samples have had a correlated trend of antibacterial activity against two bacterial strains with the positive control samples and they have showed wider inhibition zone in case of *E. coli* compared to *S. aureus* (Fig. 10).

4. Conclusion and forward-looking view

In this study, uniform and free-standing electrospun nanofibers of pullulan/tetracycline-HPβCD-IC have been obtained via electrospinning technique. The molar ratio of HPβCD:tetracycline inclusion complexes has been determined as 2:1 which has enabled to obtain homogenous nanofibrous web efficiently. A control sample of pullulan/tetracycline nanofibers have been generated, as well. Both nanofibers have been obtained with the drug loading efficiency of ∼ 100 % (w/w) supporting the efficient encapsulation potential of electrospun nanofibrous webs. On the other hand, it has been concluded from the structural analyses that the tetracycline and HPβCD successfully formed inclusion complexes that were incorporated into the nanofibers. Moreover, computational modeling study has supported our experimental findings where 2:1 M ratio (CD:drug) has found to be more favorable to form inclusion complexes between tetracycline and HPβCD when compared to 1:1 one. Due to inclusion complexation, tetracycline has been found in the amorphous state which has ensured the enhanced solubility of drug molecule encapsulated in the nanofibrous web. Additionally, faster and higher release of drug from pullulan/tetracycline-HPβCD-IC nanofibers has been attained compared to pullulan/tetracycline one. Pullulan/tetracycline-HPβCD-IC nanofibers have also disintegrated when placed in an artificial saliva environment while control sample of pullulan/tetracycline nanofibers has remained as a thin layer without complete absorption. Here, the superior properties of pullulan/tetracycline-HPβCD-IC nanofibers have been derived from the collaboration of amorphous distribution of tetracycline arising with complex formation; highly porous structure and high surface area of nanofibers; extreme aqueous solubility of HPβCD. In addition to these, pullulan/tetracycline-HPβCD-IC nanofibers have showed a promising antibacterial activity against both gram-positive (*S.aureus*) and gram-negative (*E. coli*) bacteria. The use of only water during the generation of nanofibers has been another advantage of our approach in which there was no need to use unfavorable toxic solvents or chemicals. Here, the water-soluble polymeric matrix of pullulan could be directly mixed with the inclusion complex system of tetracycline-HPβCD which has been also prepared in aqueous medium. So, the one-step preparation of the electrospinning system in water is also a non-negligible advantage of our approach especially for the industrialization of this orally disintegrating dosage formulation. Here, the notable fast-disintegrating profile of pullulan/tetracycline-HPβCD-IC nanofibers might be also a

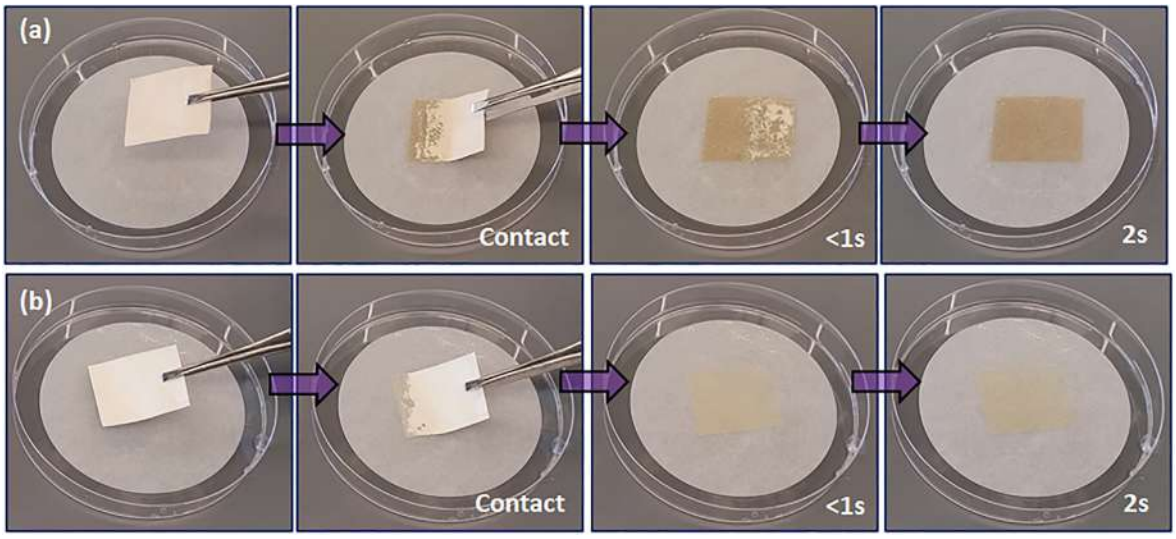

Fig. 9. Disintegration profile of (a) pullulan/tetracycline-HPβCD-IC nanofibers and (b) pullulan/ tetracycline nanofibers. The photos have been captured from the Video S1.

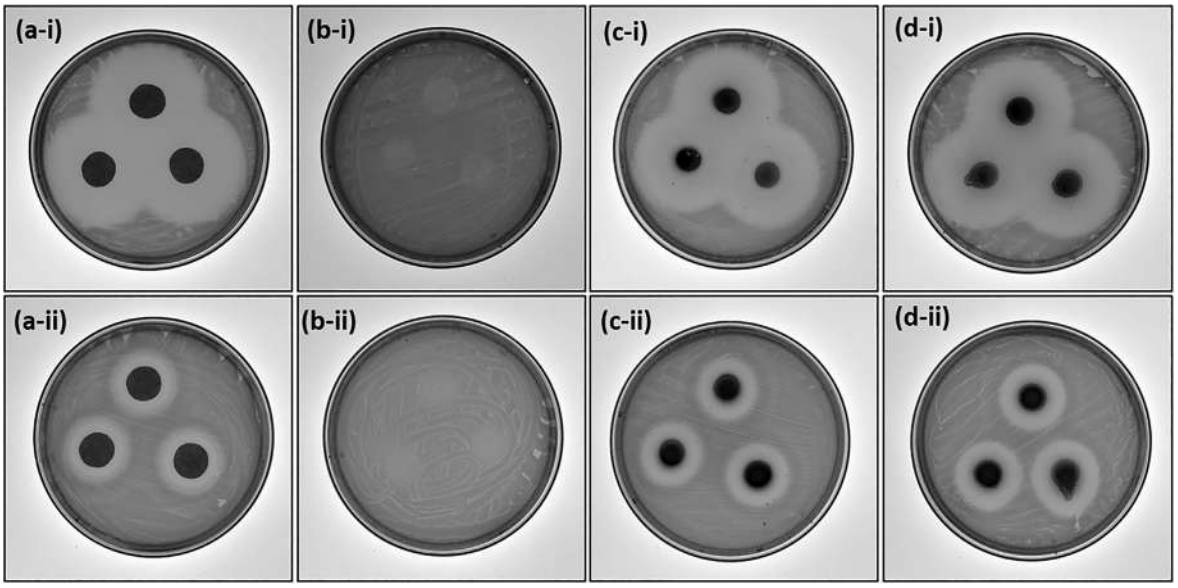

Fig. 10. Photos of antibacterial test of (a) filter paper impregnated with tetracycline solution, (b) pullulan/HPβCD nanofibers, (c) pullulan/tetracycline nanofibers, (d) pullulan/ tetracycline-HPβCD-IC nanofibers against (i) *E. coli* and (ii) *S. aureus* strains.

Table 3
The diameter of bacterial inhibition zones of samples. (Sample diameter: ~ 15 mm).

Diameter (mm)	Filter paper/ tetracycline	Pullulan/ HPβCD NF	Pullulan/ tetracycline NF	Pullulan/ tetracycline-HPβCD-IC NF
E. coli	49.86 ± 0.81	–	46.48 ± 0.23	48.91 ± 0.23
S. aureus	28.10 ± 0.46	–	26.62 ± 0.46	28.91 ± 0.46

solution against the potential graininess and the unpleasant mouthfeel that can happen by the slow disintegration of tablet dosage forms. Moreover, the flexible and free-standing properties of nanofibers might offer a remedy to the fragile and brittle feature that can be observed in the case of tablet formulations depending on the conducted production technique. Briefly, the electrospun nanofibrous webs produced by the combination of tetracycline-HPβCD-IC and water-soluble biopolymer of pullulan might be a promising alternative to conventional means of oral drug delivery systems as an orally fast disintegrating dosage formulation for an effective antibiotic treatment.

CRediT authorship contribution statement

Emmy Hsiung: Investigation, Writing – original draft. **Asli Celebioglu:** Conceptualization, Methodology, Investigation, Writing – original draft. **Rimi Chowdhury:** Investigation, Writing – original draft. **Mehmet E. Kilic:** Investigation, Writing – original draft.

Engin Durgun: Supervision, Resources, Writing – original draft. **Craig Altier:** Supervision, Resources. **Tamer Uyar:** Supervision, Conceptualization, Resources, Funding acquisition.

Declaration of Competing Interest

The authors declare that they have no known competing financial interests or personal relationships that could have appeared to influence the work reported in this paper.

Acknowledgments

This work made use of the Cornell Center for Materials Research Shared Facilities which are supported through the NSF MRSEC program (DMR-1719875), and the Cornell Chemistry NMR Facility supported in part by the NSF MRI program (CHE-1531632), and Department of Human Centered Design facilities. M.E.K acknowledges support from Brain Pool Program through the National Research Foundation of Korea (NRF) funded by the Ministry of Science and ICT (2020H1D3A1A02081517).

Appendix A. Supplementary data

Supplementary data to this article can be found online at https://doi.org/10.1016/j.jcis.2021.12.013.

References

[1] A. Singh, V.A. Ansari, F. Haider, F. Ahsan, T. Mahmood, S. Maheshwari, R.K. Tiwari, Oral fast dissolving film: The avant-garde avenue for oral consignment modus operandi, Res. J. Pharm. Technol. 14 (2021) 2145–2152.
[2] M. Preis, Orally disintegrating films and mini-tablets—innovative dosage forms of choice for pediatric use, Aaps Pharmscitech. 16 (2) (2015) 234–241.
[3] P. Baghel, A. Roy, S. Chandrakar, S. Bahadur, Fast dissolving drug delivery systems: a brief review, Res. J. Pharm. Technol. 6 (2013) 597–602.
[4] C.B.J. Manuel, V.G.L. Jesús, S.M. Aracely, Electrospinning for drug delivery systems: Drug incorporation techniques, Electrospinning-Material, Tech. Biomed. Appl. (2016) 14.
[5] M. Mehdi, S. Hussain, B. Bin Gao, K.A. Shah, F.K. Mahar, M. Yousif, F. Ahmed, Fabrication and characterization of rizatriptan loaded pullulan nanofibers as oral fast-dissolving drug system, Mater. Res. Express. 8 (2021) 55404.
[6] B. Balusamy, A. Celebioglu, A. Senthamizhan, T. Uyar, Progress in the design and development of "fast-dissolving" electrospun nanofibers based drug delivery systems - A systematic review, J. Control. Release. 326 (2020) 482–509.
[7] A. Celebioglu, T. Uyar, Electrohydrodynamic encapsulation of eugenol-cyclodextrin complexes in pullulan nanofibers, Food Hydrocoll. 111 (2021) 106264.
[8] N.N. Bailore, S.K. Balladka, S.J.D.S. Doddapaneni, M.S. Mudiyaru, Fabrication of Environmentally Compatible Biopolymer Films of Pullulan/Piscean Collagen/ZnO Nanocomposite and Their Antifungal Activity, J. Polym. Environ. 29 (2021) 1192–1201.
[9] R.Y. Lochhead, The use of polymers in cosmetic products, Cosmet. Sci. Technol. (2017) 171–221.
[10] S. Asgari, A. Pourjavadi, M. Setayeshmehr, A. Boisen, F. Ajalloueian, Encapsulation of Drug-Loaded Graphene Oxide-Based Nanocarrier into Electrospun Pullulan Nanofibers for Potential Local Chemotherapy of Breast Cancer, Macromol. Chem. Phys. 222 (2021) 2100096.
[11] H. Pang, K. Tian, Y. Li, C. Su, F. Duan, Y. Xu, Super-hydrophobic PTFE hollow fiber membrane fabricated by electrospinning of Pullulan/PTFE emulsion for membrane deamination, Sep. Purif. Technol. 274 (2021) 118186.
[12] D. Atila, D. Keskin, A. Tezcaner, Crosslinked pullulan/cellulose acetate fibrous scaffolds for bone tissue engineering, Mater. Sci. Eng. C. 69 (2016) 1103–1115.
[13] A. Celebioglu, Z.I. Yildiz, T. Uyar, Fabrication of electrospun eugenol/cyclodextrin inclusion complex nanofibrous webs for enhanced antioxidant property, water solubility, and high temperature stability, J. Agric. Food Chem. 66 (2) (2018) 457–466.
[14] E.J. Dierings de Souza, D.H. Kringel, A.R. Guerra Dias, E. da Rosa Zavareze, Polysaccharides as wall material for the encapsulation of essential oils by electrospun technique, Carbohydr. Polym. 265 (2021) 118068.
[15] M. Duan, S. Yu, J. Sun, H. Jiang, J. Zhao, C. Tong, Y. Hu, J. Pang, C. Wu, Development and characterization of electrospun nanofibers based on pullulan/chitin nanofibers containing curcumin and anthocyanins for active-intelligent food packaging, Int. J. Biol. Macromol. 187 (2021) 332–340.
[16] K.M. Soto, M. Hernández-Iturriaga, G. Loarca-Piña, G. Luna-Bárcenas, S. Mendoza, Antimicrobial effect of nisin electrospun amaranth: pullulan nanofibers in apple juice and fresh cheese, Int. J. Food Microbiol. 295 (2019) 25–32.
[17] Y. Yang, S. Zheng, Q. Liu, B. Kong, H. Wang, Fabrication and characterization of cinnamaldehyde loaded polysaccharide composite nanofiber film as potential antimicrobial packaging material, Food Packag. Shelf Life. 26 (2020) 100600.
[18] J. Teno, M. Pardo-Figuerez, N. Hummel, V. Bonin, A. Fusco, C. Ricci, G. Donnarumma, M.-B. Coltelli, S. Danti, J.M. Lagaron, Preliminary studies on an innovative bioactive skin soluble beauty mask made by combining electrospinning and dry powder impregnation, Cosmetics. 7 (2020) 96.
[19] Z.-y. Qin, X.-W. Jia, Q. Liu, B.-H. Kong, H. Wang, Fast dissolving oral films for drug delivery prepared from chitosan/pullulan electrospinning nanofibers, Int. J. Biol. Macromol. 137 (2019) 224–231.
[20] A. Costoya, A. Concheiro, C. Alvarez-Lorenzo, Electrospun fibers of cyclodextrins and poly (cyclodextrins), Molecules 22 (2017) 230.
[21] F. Topuz, T. Uyar, Electrospinning of Cyclodextrin Functional Nanofibers for Drug Delivery Applications, Pharmaceutics. 11 (2019) 6.
[22] A. Dodero, G. Schlatter, A. Hébraud, S. Vicini, M. Castellano, Polymer-free cyclodextrin and natural polymer-cyclodextrin electrospun nanofibers: A comprehensive review on current applications and future perspectives, Carbohydr. Polym. 264 (2021) 118042.
[23] C. Patiño Vidal, C. López de Dicastillo, F. Rodríguez-Mercado, A. Guarda, M.J. Galotto, C. Muñoz-Shugulí, Electrospinning and cyclodextrin inclusion complexes: An emerging technological combination for developing novel active food packaging materials, Crit. Rev. Food Sci. Nutr. (2021) 1–16.
[24] E.M.M. Del Valle, Cyclodextrins and their uses: a review, Process Biochem. 39 (9) (2004) 1033–1046.
[25] G. Crini, A history of cyclodextrins, Chem. Rev. 114 (2014) 10940–10975.
[26] A. Celebioglu, T. Uyar, Electrospun formulation of acyclovir/cyclodextrin nanofibers for fast-dissolving antiviral drug delivery, Mater. Sci. Eng. C. 118 (2021) 111514.
[27] M.E. Brewster, T. Loftsson, Cyclodextrins as pharmaceutical solubilizers, Adv. Drug Deliv. Rev. 59 (7) (2007) 645–666.
[28] Z. Aytac, H.S. Sen, E. Durgun, T. Uyar, Sulfisoxazole/cyclodextrin inclusion complex incorporated in electrospun hydroxypropyl cellulose nanofibers as drug delivery system, Colloids Surfaces B Biointerfaces. 128 (2015) 331–338.
[29] Z. Aytac, S. Ipek, I. Erol, E. Durgun, T. Uyar, Fast-dissolving electrospun gelatin nanofibers encapsulating ciprofloxacin/cyclodextrin inclusion complex, Colloids Surfaces B Biointerfaces. 178 (2019) 129–136.
[30] M.F. Canbolat, A. Celebioglu, T. Uyar, Drug delivery system based on cyclodextrin-naproxen inclusion complex incorporated in electrospun polycaprolactone nanofibers, Colloids Surfaces B Biointerfaces. 115 (2014) 15–21.
[31] S. Gould, R.C. Scott, 2-Hydroxypropyl-β-cyclodextrin (HP-β-CD): a toxicology review, Food Chem. Toxicol. 43 (10) (2005) 1451–1459.
[32] S. Gao, X. Li, J. Jiang, L. Zhao, Y. Fu, F. Ye, Fabrication and characterization of thiophanate methyl/hydroxypropyl-β-cyclodextrin inclusion complex nanofibers by electrospinning, J. Mol. Liq. 335 (2021) 116228.
[33] S. Gao, Y. Liu, J. Jiang, X. Li, F. Ye, Y. Fu, L. Zhao, Thiram/hydroxypropyl-β-cyclodextrin inclusion complex electrospun nanofibers for a fast dissolving water-based drug delivery system, Colloids Surfaces B Biointerfaces. 201 (2021) 111625.
[34] A. Celebioglu, T. Uyar, Metronidazole/Hydroxypropyl-β-Cyclodextrin Inclusion Complex Nanofibrous Webs as Fast-dissolving Oral Drug Delivery System, Int. J. Pharm. 572 (2019) 118828.
[35] A. Celebioglu, T. Uyar, Fast Dissolving Oral Drug Delivery System based on Electrospun Nanofibrous Webs of Cyclodextrin/Ibuprofen Inclusion Complex Nanofibers, Mol. Pharm. 16 (10) (2019) 4387–4398.
[36] A. Celebioglu, T. Uyar, Hydrocortisone/cyclodextrin complex electrospun nanofibers for a fast-dissolving oral drug delivery system, RSC Med. Chem. 11 (2) (2020) 245–258.
[37] A.I. Caço, F. Varanda, M.J. Pratas de Melo, A.M.A. Dias, R. Dohrn, I.M. Marrucho, Solubility of antibiotics in different solvents. Part II. Non-hydrochloride forms of tetracycline and ciprofloxacin, Ind. Eng. Chem. Res. 47 (21) (2008) 8083–8089.
[38] F. Varanda, M.J. Pratas de Melo, A.I. Caço, R. Dohrn, F.A. Makrydaki, E. Voutsas, D. Tassios, I.M. Marrucho, Solubility of antibiotics in different solvents. 1. Hydrochloride forms of tetracycline, moxifloxacin, and ciprofloxacin, Ind. Eng. Chem. Res. 45 (18) (2006) 6368–6374.
[39] A.P.F. Monteiro, C.M.S.L. Rocha, M.F. Oliveira, S.M.L. Gontijo, R.R. Agudelo, R.D. Sinisterra, M.E. Cortés, Nanofibers containing tetracycline/β-cyclodextrin: Physico-chemical characterization and antimicrobial evaluation, Carbohydr. Polym. 156 (2017) 417–426.
[40] B.S. Verza, J.J.J.P. van den Beucken, J.V. Brandt, M.J. Junior, V.A.R. Barao, R.D. Piazza, O. Tagit, D.M.P. Spolidorio, C.E. Vergani, E.D. de Avila, A long-term controlled drug-delivery with anionic beta cyclodextrin complex in layer-by-layer coating for percutaneous implants devices, Carbohydr. Polym. 257 (2021) 117604.
[41] J.M. Moreno-Cerezo, M. Córdoba-Díaz, D. Córdoba-Díaz, M. Córdoba-Borrego, A stability study of tetracycline and tetracycline cyclodextrins in tablets using a new HPLC method, J. Pharm. Biomed. Anal. 26 (3) (2001) 417–426.

[42] C. Ulker Turan, A. Metin, Y. Guvenilir, Controlled release of tetracycline hydrochloride from poly (ω-pentadecalactone-co-ε-caprolactone)/gelatin nanofibers, Eur. J. Pharm. Biopharm. 162 (2021) 59–69.
[43] L. Behbood, S. Karimi, E. Mirzaei, G. Mohammadi, M. Azami, E. Arkan, Mucoadhesive chitosan electrospun nanofibers containing tetracycline and triamcinolone as a drug delivery system, Fibers Polym. 19 (7) (2018) 1454–1462.
[44] N. Sultana, A. Zainal, Cellulose acetate electrospun nanofibrous membrane: fabrication, characterization, drug loading and antibacterial properties, Bull. Mater. Sci. 39 (2016) 337–343.
[45] Y.J. Son, Y. Kim, W.J. Kim, S.Y. Jeong, H.S. Yoo, Antibacterial nanofibrous mats composed of Eudragit for pH-dependent dissolution, J. Pharm. Sci. 104 (8) (2015) 2611–2618.
[46] N. Alhusein, I.S. Blagbrough, M.L. Beeton, A. Bolhuis, P.A. De Bank, Electrospun zein/PCL fibrous matrices release tetracycline in a controlled manner, killing Staphylococcus aureus both in biofilms and ex vivo on pig skin, and are compatible with human skin cells, Pharm. Res. 33 (1) (2016) 237–246.
[47] N. Nematpour, N. Farhadian, K.S. Ebrahimi, E. Arkan, F. Seyedi, S. Khaledian, M. Shahlaei, S. Moradi, Sustained release nanofibrous composite patch for transdermal antibiotic delivery, Colloids Surfaces A Physicochem. Eng. Asp. 586 (2020) 124267.
[48] M. Abdoli, K. Sadrjavadi, E. Arkan, M.M. Zangeneh, S. Moradi, A. Zangeneh, S. Khaledian, Polyvinyl alcohol/Gum tragacanth/graphene oxide composite nanofiber for antibiotic delivery, J. Drug Deliv. Sci. Technol. 60 (2020) 102044.
[49] M. Ghorbani, F. Mahmoodzadeh, L. Yavari Maroufi, P. Nezhad-Mokhtari, Electrospun tetracycline hydrochloride loaded zein/gum tragacanth/poly lactic acid nanofibers for biomedical application, Int. J. Biol. Macromol. 165 (2020) 1312–1322.
[50] E.-R. Kenawy, G.L. Bowlin, K. Mansfield, J. Layman, D.G. Simpson, E.H. Sanders, G.E. Wnek, Release of tetracycline hydrochloride from electrospun poly (ethylene-co-vinylacetate), poly (lactic acid), and a blend, J. Control. Release. 81 (1-2) (2002) 57–64.
[51] W. Kohn, L.J. Sham, Self-consistent equations including exchange and correlation effects, Phys. Rev. 140 (4A) (1965) A1133–A1138.
[52] P. Hohenberg, W. Kohn, Inhomogeneous electron gas, Phys. Rev. 136 (3B) (1964) B864–B871.
[53] G. Kresse, J. Furthmüller, Efficient iterative schemes for ab initio total-energy calculations using a plane-wave basis set, Phys. Rev. B. 54 (1996) 11169.
[54] J.P. Perdew, K. Burke, M. Ernzerhof, Generalized gradient approximation made simple [Phys. Rev. Lett. 77, 3865 (1996)], Phys. Rev. Lett. 78 (1997) 1396.
[55] S. Grimme, Semiempirical GGA-type density functional constructed with a long-range dispersion correction, J. Comput. Chem. 27 (15) (2006) 1787–1799.
[56] P.E. Blöchl, Projector augmented-wave method, Phys. Rev. B. 50 (24) (1994) 17953–17979.
[57] K. Mathew, R. Sundararaman, K. Letchworth-Weaver, T.A. Arias, R.G. Hennig, Implicit solvation model for density-functional study of nanocrystal surfaces and reaction pathways, J. Chem. Phys. 140 (2014) 84106.
[58] Y. Bi, H. Sunada, Y. Yonezawa, K. Danjo, A. Otsuka, K. Iida, Preparation and evaluation of a compressed tablet rapidly disintegrating in the oral cavity, Chem. Pharm. Bull. 44 (11) (1996) 2121–2127.
[59] T. Higuchi, K.A. Connors, Phase solubility diagram, Adv Anal Chem Instrum. 4 (1965) 117–212.
[60] T. Uyar, F. Besenbacher, Electrospinning of uniform polystyrene fibers: The effect of solvent conductivity, Polymer (Guildf). 49 (24) (2008) 5336–5343.
[61] M.A. Watson, J.M. Lea, K.L. Bett-Garber, Spray drying of pomegranate juice using maltodextrin/cyclodextrin blends as the wall material, Food Sci. Nutr. 5 (3) (2017) 820–826.
[62] A. Celebioglu, T. Uyar, Development of ferulic acid/cyclodextrin inclusion complex nanofibers for fast-dissolving drug delivery system, Int. J. Pharm. 584 (2020) 119395, https://doi.org/10.1016/j.ijpharm.2020.119395.
[63] C. Yuan, B. Liu, H. Liu, Characterization of hydroxypropyl-β-cyclodextrins with different substitution patterns via FTIR, GC–MS, and TG–DTA, Carbohydr. Polym. 118 (2015) 36–40.
[64] P. Shao, B. Niu, H. Chen, P. Sun, Fabrication and characterization of tea polyphenols loaded pullulan-CMC electrospun nanofiber for fruit preservation, Int. J. Biol. Macromol. 107 (2018) 1908–1914.
[65] M.K. Trivedi, S. Patil, H. Shettigar, K. Bairwa, S. Jana, Spectroscopic characterization of chloramphenicol and tetracycline: an impact of biofield treatment, Pharm. Anal. Acta. 6 (2015) 395.
[66] P. Mura, Analytical techniques for characterization of cyclodextrin complexes in the solid state: A review, J. Pharm. Biomed. Anal. 113 (2015) 226–238.
[67] N.A. Peppas, B. Narasimhan, Mathematical models in drug delivery: How modeling has shaped the way we design new drug delivery systems, J. Control. Release. 190 (2014) 75–81.
[68] X. Li, M.A. Kanjwal, L. Lin, I.S. Chronakis, Electrospun polyvinyl-alcohol nanofibers as oral fast-dissolving delivery system of caffeine and riboflavin, Colloids Surfaces B Biointerfaces. 103 (2013) 182–188.
[69] E.E. Ozseker, A. Akkaya, Development of a new antibacterial biomaterial by tetracycline immobilization on calcium-alginate beads, Carbohydr. Polym. 151 (2016) 441–451.
[70] T.H. Grossman, Tetracycline antibiotics and resistance, Cold Spring Harb. Perspect. Med. 6 (4) (2016) a025387, https://doi.org/10.1101/cshperspect.a025387.
[71] S.M. Heman-Ackah, Comparison of tetracycline action on Staphylococcus aureus and Escherichia coli by microbial kinetics, Antimicrob. Agents Chemother. 10 (2) (1976) 223–228.